1 Liquid-Liquid Equilibria of Water + Ethanol + Castor Oil

and the Effect of Cellulose Nanocrystal/Fe₃O₄ and

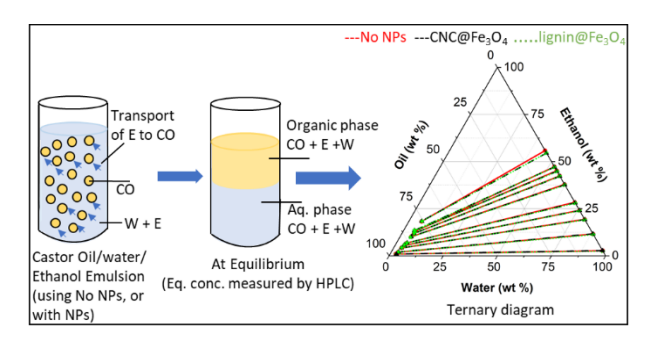
3 Lignin/Fe₃O₄ Nanoparticles

- 5 Mohammad J. Hasan^a, Fariba Yeganeh^{a,b}, Amy Ciric^c, Peng Chen^c, Erick S. Vasquez^{c,d}, Esteban E.
- *Ureña-Benavides*^{a*}
- 7 ^aDepartment of Biomedical Engineering and Chemical Engineering, The University of Texas at San
- 8 Antonio, One UTSA Circle, San Antonio, 78249, TX, USA.
- 9 bSustainable Polymer & Innovative Composite Materials Research Group, Department of Chemistry,
- 10 Faculty of Science, King Mongkut's University of Technology Thonburi, 126 Pracha Uthit Road,
- 11 Bangmod, Thungkru, Bangkok, 10140, Thailand.
- ^cDepartment of Chemical and Materials Engineering, University of Dayton, 300 College Park, Dayton,
- 13 OH, 45469-0256, USA.

dIntegrative Science and Engineering Center, University of Dayton, 300 College Park, Dayton, OH,
 45469, USA.

ABSTRACT

Castor oil has been proposed as a renewable solvent for the liquid extraction of ethanol from water as an alternative to more traditional energy intensive distillation-based methods. The liquid-liquid equilibrium (LLE) of the ternary system water + ethanol + castor oil was determined at 295.15 K using high performance liquid chromatography (HPLC). Castor oil was herein treated as a pseudo-component with the molecular weight of the triglyceride of ricinoleic acid. The experimental data was fitted to the UNIQUAC and NRTL models to obtain parameters for castor oil, and binary interaction parameters for castor oil/ethanol and castor oil/water pairs. The separation factors and distribution coefficients of water and ethanol were calculated at ethanol concentrations ranging from 2.73 ± 0.35 to 55.8 ± 1.1 wt%, with a high separation factor of 12.7 ± 3.3 , and a distribution coefficient of 0.352 ± 0.078 , at the lowest ethanol concentration tested. Moreover, iron oxide-coated cellulose nanocrystals (CNC@Fe₃O₄) and Kraft lignin-coated iron oxide (lignin@Fe₃O₄) nanoparticles (NPs) were added to the castor oil + water + ethanol mixtures at 0.01 g/g mixture, to investigate the effect of the NPs in altering the LLE of the system. It was found that the NPs had a negligible (<1%) effect on the thermodynamic equilibrium, which opens the possibility of using them in advanced applications such as the magnetically controlled demulsification of stable dispersions generated during liquid-liquid extraction process.



KEYWORDS: Liquid-liquid equilibria; Ternary diagram; Water + Ethanol + Castor oil; LLE; Ethanol Extraction.

1. Introduction

Anhydrous ethanol produced by fermenting renewable substrates is a promising sustainable and environmentally friendly fuel [1]. However, fermentation produces dilute aqueous solutions of ethanol, and recovering it from such homogenous mixtures is a significant challenge. Although distillation is a common method for recovering ethanol from aqueous solutions, the energy needs for the separation can be considerable [1–3]. Moreover, the azeotrope represents an additional complication in the ethanol-water distillation and necessitates additional processing by azeotropic or extractive distillation, adsorption, or pervaporation in order to produce an anhydrous product [2,3]. Liquid—liquid solvent extraction, an appealing alternate separation procedure for ethanol, has the potential of being more energy efficient than distillation [4].

Extraction solvents are often chosen based on extraction performance, aqueous feed solubility, chemical stability, phase immiscibility, cost of the solvent, product separation, and safety hazards to humans and the environment [5]. Unfortunately, there is no ideal solvent that fulfills all these criteria. Therefore, a compromise must be made. Based on the ethanol distribution coefficients, Munson and King [6] ranked the solvent classes as follows: hydrocarbons < ethers < ketones < amines < esters < alcohols < carboxylic acids. Alcohols, esters, and ketones are desirable because their distribution coefficients are greater than ethers and hydrocarbons as well as being less reactive than amines and carboxylic acids. The main problem has been the toxicity of extraction solvents, which has led to the elimination of the majority of solvents of interest in the lower molecular weight range. Mehta and Fraser [7] proposed using higher molecular weight hydrocarbons and vegetable oils for the extraction of ethanol. They evaluated cottonseed oil, hexadecane and paraffin oil, and provided extraction data for paraffin oil. Offeman et al. [5] investigated a variety of vegetable oils such as castor oil, coconut oil, olive oil, and safflower oil to extract ethanol from an initial aqueous ethanol concentration of 5 wt%. Plant based oils used as solvents for liquid-liquid extraction of ethanol have shown high distribution coefficients and separation factors [5]. Most vegetable oils are complex mixtures of multiple components; however, they can be approximated as a single pseudocomponent, allowing the liquid-liquid equilibrium to be visualized on a ternary diagram and simplifying models for preliminary design of liquid/liquid extraction processes. A similar approach was taken by Ghosh et al., where they used neem oil as a pseudo-component and developed {water + surfactant + neem oil} pseudo ternary diagrams for the extraction of surfactants from water [8]. Franca et. al [9] studied liquid-liquid equilibria for castor oil biodiesel + glycerol + alcohols and developed a pseudo ternary diagram where biodiesel was represented by methyl ricinoleate, the major component of castor oil biodiesel. Moreover, Oliveira et al. [10] investigated various LLE systems containing acylglycerols from olive oil,

glycerol and isopropanol. Voll et al. [11] reported the LLE for the system (hydrolyzed palm oil + ethanol + water) for diacylglycerol enrichment.

 Castor oil is a naturally occurring vegetable oil produced from the seeds of the castor bean plant, *Ricinus communis*. It has been used in many applications as a chemical feedstock [12], lubricant [12], biodiesel raw material [13], coating [14], paint medium [15], and extraction solvent [5]. Most vegetable oils are used for food products; however, castor oil, a natural laxative, is not typically used for such purposes. Several research papers have characterized castor oil and identified its components using high performance liquid chromatography (HPLC) [16–18]. It is primarily composed of triglycerides of ricinoleic acid [19], but it also contains smaller amounts of other fatty acids such as stearic acid, palmitic acid, oleic acid, linolenic acid, and linoleic acid [12,19]. Like all fatty acids, ricinoleic acid has a carboxylic head that reacts with glycerol to form a triglyceride. However, it also has a second hydroxyl group, making castor oil slightly more polar than most vegetable oils and an attractive solvent for ethanol recovery. Castor oil's high ethanol affinity, immiscibility with water, limited toxicity, low volatility, low heat capacity, low environmental impact, and low price make it an attractive candidate as a renewable solvent. For these reasons, in this work castor oil is chosen over other solvents.

Cellulose and lignin based NPs have been employed in Pickering emulsions by various authors [20–24]. Combining cellulose and lignin-based NPs with Fe₃O₄ NPs makes the hybrid NPs superparamagnetic which can be useful to control the stability of three-component Pickering emulsion system, and to enhance coalescence and mass transfer for liquid-liquid extraction in the presence of a magnetic field [20]. Moreover, after an appropriate separation is done, the magnetic NPs may be recovered and recycled. In our recent publication [20], we developed magnetically-controllable castor oil/water Pickering emulsions that were stabilized by Fe₃O₄-coated cellulose nanocrystals (CNC@Fe₃O₄). Later, we developed magnetically-controllable three-component castor oil/water/ethanol Pickering emulsions, stabilized by CNC@Fe₃O₄ and lignin@Fe₃O₄ NPs, for the extraction of ethanol from aqueous solutions into castor oil [25]. However, further development of this process requires characterizing the LLE of the castor oil/water/ethanol ternary mixtures so that the amount of ethanol that can be extracted at a given {castor oil + water + ethanol} composition can be determined. Moreover, it is also needed to study the effect of the NPs on castor oil/water/ethanol LLE to establish if the particles have any effect on the thermodynamic equilibrium.

In this work, experimental liquid-liquid equilibrium data of the ternary system {water + ethanol + castor oil} was determined for the first time at a wide range of initial ethanol concentrations (3 to 55 wt%) at 295.15 K, with and without NPs. The equilibrium concentrations were measured via HPLC. The liquid-liquid equilibrium behavior is presented on ternary diagrams, which conveniently depict the system's behavior and are often used to design solvent extraction equipment and processes. The experimental data herein obtained was also fitted to the nonrandom two-liquid (NRTL) and the universal quasichemical (UNIQUAC) liquid phase activity models, yielding parameter values for castor oil, and for castor oil/water and castor oil/ethanol binary pairs [26–28]. This modeling was done by treating castor oil as a pseudocomponent, leading to three-component models of the LLE that can be visualized on a ternary diagram and easily implemented for preliminary process design. Furthermore, the distribution coefficients and separation factors of ethanol were calculated from experimental data to quantify the efficacy of castor oil in extracting ethanol from aqueous solutions. In addition, Fe₃O₄-coated cellulose nanocrystals (CNC@Fe₃O₄) and lignin-coated Fe₃O₄ (lignin@Fe₃O₄) nanocomposites were added separately to water/ethanol/castor-oil mixtures to study their effect on the LLE.

2. Experimental

2.1. Materials

The relevant information of the chemicals used in this work is shown in Table 1. The chemicals were used as received without any additional treatment. Castor oil (batch number: MKCP1892) was purchased from Sigma Aldrich. Since castor oil is a complex mixture, the oil purity was measured by Karl-Fisher titration to determine water content and subtract the amount of oil. Southern Bleached Softwood Kraft (SBSK) pulp cellulose was kindly donated by Weyerhaeuser pulp mill (Columbus, MS) as a cellulosic source for the synthesis of cellulose nanocrystals. The purity of SBSK pulp was determined by measuring the solid content using a gravimetric method. Kraft lignin (Lot # MKCG9481) was purchased from Sigma Aldrich.

Table 1. Relevant information of the materials

Chemical name	CAS no.	IUPAC Name	Supplier	Mass purity	Purity Analysis Method
Water	7732-18-5	oxidane	Fisher Scientific	99.9 %	as stated by the supplier
2-propanol	67-63-0	propan-2-ol	Fisher Scientific	99.9 %	as stated by the supplier
Methanol	67-56-1	methanol	Fisher Scientific	99.9 %	as stated by the supplier
Hexane	110-54-3	hexane	Fisher Scientific	98.5 %	as stated by the supplier
Ethanol	64-17-5	ethanol	Fisher Scientific	99.5%	as stated by the supplier
Ammonium Hydroxide	1336-21-6	ammonium hydroxide	Fisher Scientific	28.0 - 30.0 %	as stated by the supplier
Iron (II) chloride tetrahydrate	13478-10-9	dichloroiron tetrahydrate	Fisher Scientific	96.0 %	as stated by the supplier
Iron (III) chloride hexahydrate	10025-77-1	trichloroiron; hexahydrate	Fisher Scientific	97.0 %	as stated by the supplier
Castor oil	8001-79-4	-	Sigma Aldrich	99.80 %	KF titration
Southern bleached	_	-	Weyerhaeuser	94.62 %	gravimetric
softwood Kraft			pulp mill		method
pulp cellulose			(Columbus, MS).		
Kraft lignin	8068-05-1	-	Sigma Aldrich	95.0 %	as stated by the supplier
Sulfuric acid	7664-93-9	sulfuric acid	Fisher Scientific	95.0 – 98.0 %	as stated by the supplier
Acetic acid	64-19-7	acetic acid	Fisher Scientific	99.0 %	as stated by the supplier

2.2. Synthesis of CNC@ Fe_3O_4 and lignin@ Fe_3O_4 nanocomposites

Cellulose nanocrystals were first prepared in-house using a widely known acid hydrolysis method with sulfuric acid [29]. In short, Southern Bleached Softwood Kraft pulp cellulose was hydrolyzed using 64% sulfuric acid at a cellulose to sulfuric acid ratio of 1 g:17.5 ml at 45 °C for 50 minutes. The resulting cellulose nanocrystals (CNC) were washed with water to remove excess acid using centrifugation and

dialysis. The CNC@Fe₃O₄ nanocomposites were then prepared through a procedure described in our previous publication [20]. Briefly, Fe₃O₄ nanoparticles were synthesized through the one-step coprecipitation of iron chloride salts by ammonium hydroxide in the presence of CNC with a CNC to Fe₃O₄ mass ratio of 1:4 [20]. A detailed procedure of the synthesis of cellulose nanocrystals and CNC@Fe₃O₄ is provided in the supplementary material (SM) section 1.1. Lignin@Fe₃O₄ nanocomposites were prepared following a procedure discussed in Westphal's thesis [30]. In that case, Fe₃O₄ NPs were synthesized first and then coated with Kraft lignin (a detailed procedure is found in the SM section 1.2).

2.3. Preparation of castor oil/water/ethanol mixtures for LLE study

142

143

144145

146

147

148149150

151

152153

154

155

156 157

158

159

160 161

162

163164

165 166

167

168

169 170

171172

173

174175

176

177178

179

180

Castor oil, water, and ethanol were mixed at various compositions within the biphasic region (SM, Table S1) to prepare LLE samples of 20 g each. At first, the required amount of water was weighed and added to a centrifuge tube, followed by the addition of the corresponding amounts of ethanol and castor oil. In each sample, equal masses of castor oil and water were added, and the composition of ethanol was increased gradually. Once water, ethanol, and castor oil were combined, they were mixed with a high shear mixer (IKA Ultra-Turrax T-25 Basic, Atkinson, NH) at 10,000 rpm for 10 minutes. The mixtures were then allowed to equilibrate for 48 hours in a temperature-controlled environment at 22 ° C. The temperature was recorded over 48 hours and provided in the SM (Section 2.3 and Figure S11). After 48 hours, the emulsions had mostly phase separated, however, they were centrifuged using a benchtop centrifuge (model 5804 R, Eppendorf, Hamburg, Germany) at 11000 rpm to further complete the phase separation. Samples were taken from each phase and the concentrations of castor oil and ethanol were measured using an HPLC (model 1260 Infinity II, Agilent, Santa Clara, CA) with a multi wavelength detector (MWD). The water concentration in each phase was then calculated by mass balance. The castor oil, water, and ethanol mixtures were prepared in triplicate and the concentration of castor oil, water, and ethanol were measured using HPLC. The standard uncertainties of the measurements were calculated using the law of propagation of uncertainty according to existing literature [31,32]. The equations regarding the uncertainty calculations are provided in the SM (Section 2.4). A graphic representation of the general procedure for the preparation of castor oil/water/ethanol mixtures is shown in Figure 1. Images of the initial water/ethanol/castor oil mixtures, and after equilibrium and phase separation are provided in the SM Figure S1. It should be noted that in this study, 48 hours is enough to reach equilibrium. A detailed procedure of the test and results are provided in the SM (Section 2.1, 2.2 and Figures S9 and S10).

To study the effect of CNC@Fe₃O₄ and lignin@Fe₃O₄ NPs on water/ethanol/castor oil ternary LLE, 0.2 g CNC/Fe₃O₄ or lignin@Fe₃O₄ were dispersed in water, followed by the addition of ethanol and castor oil. The compositions of water, ethanol, and castor oil were maintained exactly the same as without NPs, as well as the procedure to reach equilibrium. Once the mixtures reached equilibrium, the phases were separated by centrifugation and the NPs were filtered out after sampling from each phase, using a syringe filter (0.45 μ m). Images of the initial water/ethanol/castor oil/ nanoparticles mixtures, and after phase separation are provided in the SM Figure S2.

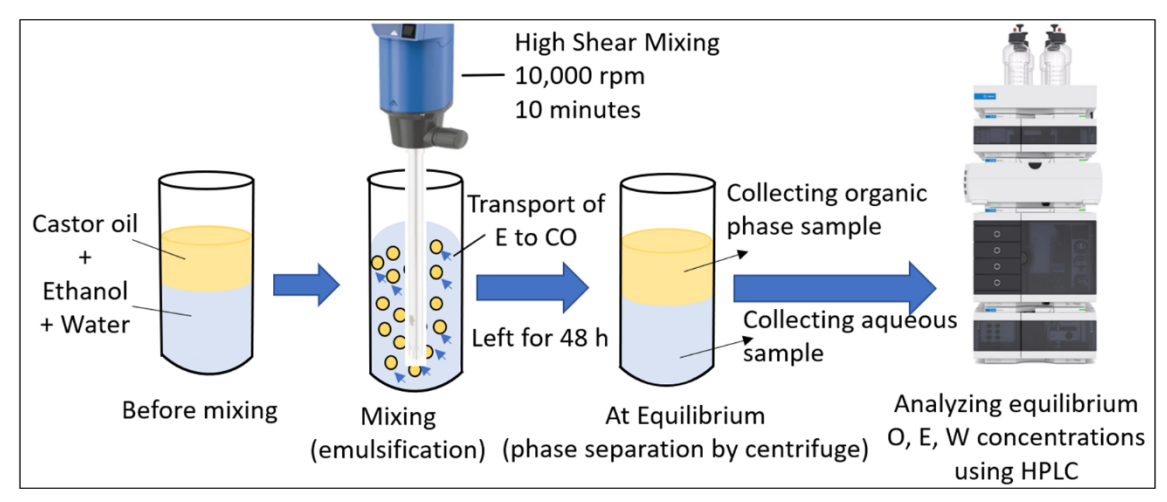


Figure 1. Schematic representation of castor oil/water/ethanol mixtures preparation for LLE studies.

2.4. Preparation of oil and aqueous phase samples for HPLC

To prepare the oil phase samples, 0.2 g were taken from the oil phase of the castor oil/water/ethanol mixture and poured into an HPLC vial (size 2 ml), followed by the addition of 0.8 g methanol. To prepare aqueous phase HPLC samples, 1 g was taken from the aqueous phase and poured into an HPLC vial without diluting in methanol.

2.5. Development of HPLC methods and calibration

To accurately quantify the castor oil, ethanol, and water concentration, two HPLC methods were developed. Method-1 provided a faster separation and measurement of equilibrium ethanol and oil concentrations. It used 100% water as the mobile phase for the first 3 minutes, followed by a gradient of water and isopropanol (IPA) for 5 minutes and 100% IPA for another 7 minutes (SM Table S2). Method-2 was comparatively slower but provided distinct peaks for multiple castor oil components. Water, methanol, and IPA were used in combinations as the mobile phases in method-2 (SM Table S3). To measure oil, ethanol, and water content in the aqueous and organic phases, a series of calibrations were conducted with known concentrations of all three components (calibration curves provided in SM Figures S3, S4, S5 and S6). By virtue of the MWD, two different wavelengths were chosen to analyze the samples; the concentration of ethanol was quantified in both methods by analyzing the ethanol peak at 192 nm, and castor oil's concentration was calculated from its corresponding peaks at 270 nm. The water content in each phase was calculated from a mass balance.

2.6. Development of castor oil/water/ethanol LLE ternary diagram

The equilibrium concentrations were plotted on three-phase ternary diagrams using the software Origin (version OriginPro 2021, OriginLab, Northampton, Massachusetts). The tie lines were obtained by connecting the corresponding aqueous phase and organic phase concentrations.

2.7. Development of UNIQUAC AND NRTL model

The UNIQUAC and NRTL parameters for the castor-oil pseudo-component in mixtures of ethanol, water, and castor oil were estimated with a least-squares fit of the experimental data, subject to the iso-activity model, mole fraction summation equations, and the model-specific equations for the liquid phase activity coefficients. This nonlinear optimization problem (NLP) was solved with a demonstration version of GAMS Studio 25.1.3, using the NLP solver CONOPT. The stability of each fitted tie line was checked

with a tangent-plane stability test implemented in Excel. The molecular weight of castor oil was approximated to that of the triglyceride of ricinoleic acid, 984.4 g/mol.

217218219

216

3. Results and Discussion

220 221

222

223224

225

226 227

228

229

230 231

232

3.1. HPLC analysis methods

The equilibrium concentrations of castor oil, ethanol, and water in the aqueous and organic phases were measured using two different HPLC methods, which differ only by how the castor oil concentrations were measured. Figure 2 shows some example chromatographs of ethanol and castor oil in the aqueous and organic phases using method 1 and method 2. In both methods, the ethanol concentrations were determined using 100% water as the mobile phase for 2 minutes and calculating the peak area at the retention time of 1.5 min. and a UV detection wavelength of 192 nm. Figure 2a shows an example HPLC chromatograph for 20% ethanol in water, and a chromatograph for 7.5% ethanol in the organic phase is shown in Figure 2d. In the latter case, the first peak at 1.25 min. was for methanol and the second peak at 1.75 min. was for ethanol. It is noted that the methanol peak appeared because the organic phase samples were diluted four times with methanol to enhance their solubility before injecting them into the HPLC. Chromatographs of ethanol in the aqueous and organic phases for method 2 were obtained using the same procedure as method 1 and are not shown in Figure 2.

233234235

236

237238

239

240

241

242

243244

245

246

247248

249

250

Castor oil is actually a mixture of multiple components [12,33,34], but may be treated as a pseudocomponent when the oil is being considered as a solvent for liquid-liquid extraction. Consequently, it is necessary to quantify the amount of oil in each phase. Two different analysis methods were used for this. In method 1, after 3 minutes, the mobile phase was switched from 100% water to a gradient of water and isopropanol (IPA) for 5 minutes, followed by 100% IPA for another 7 minutes. Most components in castor oil eluted at approximately the same time, showing only two large peaks preceded by two smaller ones. However, ethanol was effectively separated from the oil since it eluted with water before the addition of IPA as a mobile phase. All oil peaks appeared within retention times of 9 to 12 min at a wavelength of 270 nm. The concentration of castor oil was calculated from the sum of all 4 castor oil peak areas. Chromatographs of castor oil in the aqueous and organic phases measured with method 1 are shown in Fig 2b and Fig 2e, respectively. In method 2, after an initial 2 minutes of 100% water, the mobile phase was switched to a gradient of 0.5 wt% acetic acid in water and methanol as the mobile phase. In this case, most castor oil components separated and appeared as spread out peaks over retention times from 20 to 70 min. The concentration of castor oil was determined from the 2 most significant castor oil peaks at retention times from 50 to 55 min. Figure 2c and 2f show the chromatographs of castor oil in the aqueous and organic phases, respectively.

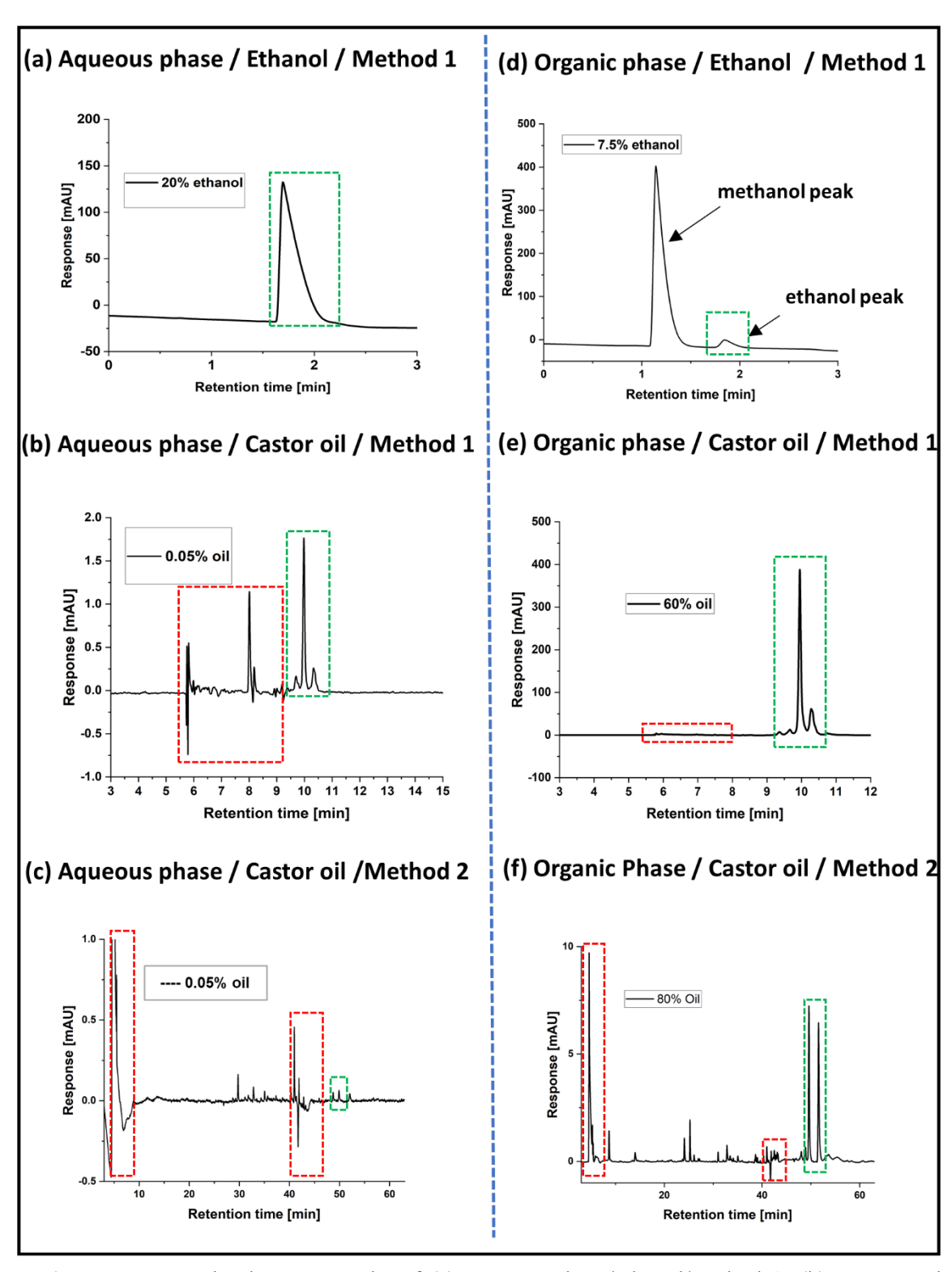


Figure 2. HPLC example chromatographs of (a) aqueous phase/ethanol/method 1; (b) aqueous phase/castor oil/method 1; (c) aqueous phase/castor oil/method 2; (d) organic phase/ethanol/method 1; (e) organic phase/castor oil/method 1; and (f) organic phase/castor oil/method 2. The peak/s inside the green dashed rectangles were considered for calculations. The peaks (signals) inside the red dashed rectangles were due to solvent switching.

259

260

261 262

263

3.2. Experimental LLE Data

The experimental LLE data of the {water + ethanol + castor oil} ternary system, at 295.15 K, is listed in Table 2. The subscripts 1, 2, and 3 represent water, ethanol, and castor oil, respectively. The compositions are provided as mass percentage (wt %). The distribution coefficients (D), and separation factors (S) of ethanol were evaluated by equations 1 to 3 [26].

264
$$D_1 = \frac{w_1^{org}}{w_1^{aq}}$$
 (1)
265 $D_2 = \frac{w_2^{org}}{w_2^{aq}}$ (2)
266 $S = \frac{D_2}{D_1}$ (3)

$$265 D_2 = \frac{w_2^{org}}{w_a^{aq}} (2)$$

$$266 S = \frac{D_2}{D_1} (3)$$

267 268

269

270 271 Where D_1 and D_2 are the distribution coefficients of water and ethanol, respectively; w_1 is the water mass fraction, and w_2 is the ethanol mass fraction. The superscripts org and aq refer to the organic and aqueous phases, respectively. The separation factor S represents the ability of castor oil to extract ethanol from water into the oil phase. Calculated values are provided in Table 3 and Figure 3.

272 273 274

275

276

277

Table 2. Experimental LLE Mass (wt%) Obtained Using the HPLC for the Ternary System of {Water (1) + Ethanol (2) + Castor Oil (3)} at T = 295.15 K and at 101.2 kPa. It is noted that w is mass percentage. The uncertainties inside the Table are standard deviations of the mean.

Method	Sample	Organic phase	·		Aqueous phas	Aqueous phase		
	Number	w_I	w_2	W3	w_I	w_2	<i>W</i> 3	
Method-1	1	2.67 ± 0.16	0.95 ± 0.13	96.38 ± 0.10	97.27 ± 0.35	2.73 ± 0.35	0.0020 ± 0.0006	
	2	3.27 ± 0.72	1.96 ± 0.15	94.77 ± 0.59	88.40 ± 0.80	11.59 ± 0.80	0.0029 ± 0.0008	
	3	3.66 ± 0.84	4.14 ± 0.03	92.20 ± 0.83	80.65 ± 0.66	19.35 ± 0.66	0.0034 ± 0.0011	
	4	4.31 ± 0.86	5.51 ± 0.25	90.18 ± 0.88	75.9 ± 1.3	24.1 ± 1.3	0.0045 ± 0.0013	
	5	4.82 ± 0.17	6.77 ± 0.25	88.40 ± 0.13	71.61 ± 0.40	28.39 ± 0.40	0.0064 ± 0.0014	
	6	5.17 ± 0.84	10.10 ± 0.19	84.72 ± 0.84	62.12 ± 0.90	37.87 ± 0.91	0.0105 ± 0.0040	
	7	5.54 ± 0.84	11.82 ± 0.08	82.64 ± 0.77	57.6 ± 1.1	42.4 ± 1.1	0.0123 ± 0.0040	
	8	5.31 ± 0.51	13.13 ± 0.42	81.56 ± 0.35	54.86 ± 0.84	45.13 ± 0.85	0.0168 ± 0.0033	
	9	5.79 ± 0.40	13.21 ± 0.15	81.00 ± 0.28	52.7 ± 1.0	47.2 ± 1.0	0.0204 ± 0.0064	
	10	5.96 ± 0.78	18.22 ± 0.19	75.83 ± 0.67	44.1 ± 1.1	55.8 ± 1.1	0.0529 ± 0.0064	
Method-2	1	2.62 ± 0.48	1.48 ± 0.57	95.89 ± 0.08	97.52 ± 0.05	2.48 ± 0.05	0.000013 ± 0.0000	
	2	2.83 ± 0.51	2.22 ± 0.77	94.95 ± 0.26	87.4 ± 1.3	12.6 ± 1.3	0.000032 ± 0.0000	
	3	2.98 ± 0.46	3.77 ± 0.36	93.25 ± 0.10	79.2 ± 2.0	20.8 ± 2.0	0.000040 ± 0.0000	
	4	3.48 ± 0.50	5.82 ± 0.25	90.70 ± 0.28	75.0 ± 1.4	25.0 ± 1.4	0.000051 ± 0.0000	
	5	3.69 ± 0.57	7.64 ± 0.35	88.67 ± 0.24	70.4 ± 2.5	29.6 ± 2.5	0.000075 ± 0.0000	
	6	4.30 ± 0.56	10.08 ± 0.49	85.61 ± 0.14	61.9 ± 1.4	39.6 ± 3.0	0.000142 ± 0.0000	
	7	4.56 ± 0.79	11.42 ± 0.81	84.01 ± 0.36	57.2 ± 1.6	44.0 ± 2.5	0.000290 ± 0.0000	
	8	4.89 ± 0.60	12.10 ± 0.44	83.01 ± 0.21	54.7 ± 1.2	46.8 ± 3.6	0.000383 ± 0.0000	
	9	4.98 ± 0.61	12.75 ± 0.23	82.27 ± 0.40	51.6 ± 2.4	48.9 ± 3.2	0.00135 ± 0.00017	
	10	5.47 ± 0.40	15.33 ± 0.42	79.19 ± 0.19	45.9 ± 1.5	55.0 ± 0.2	0.00288 ± 0.00093	

^a The standard uncertainties are calculated by using the law of propagation of uncertainty. Standard uncertainties u are u(T) = 0.30 K; u(p) = 0.1 kPa; Method-1: $u(w_1, \text{ org}) = 0.33$; $u(w_2, \text{ org}) = 0.10$; $u(w_3, \text{ org}) = 0.1$ = 0.31; $u(w_1, aq) = 0.48$; $u(w_2, aq) = 0.48$; $u(w_3, aq) = 0.0017$; Method-2: $u(w_1, org) = 0.30$; $u(w_2, org) = 0.48$; $u(w_3, aq) = 0.48$; $u(w_3, aq) = 0.0017$; Method-2: $u(w_1, org) = 0.30$; $u(w_2, org) = 0.48$; $u(w_3, aq) = 0.48$; $u(w_3, aq) = 0.0017$; Method-2: $u(w_1, org) = 0.30$; $u(w_2, org) = 0.48$; $u(w_3, aq) = 0.0017$; Method-2: $u(w_3, aq) = 0.30$; $u(w_3, aq) = 0.48$; $u(w_3, aq) = 0.0017$; Method-2: $u(w_3, aq) = 0.30$; $u(w_3, aq) = 0.48$; $u(w_3, aq) = 0.0017$; Method-2: $u(w_3, aq) = 0.30$; $u(w_3, aq) = 0.48$; $u(w_3, aq) = 0.0017$; $u(w_3, aq) = 0.30$; $u(w_3, aq) = 0.30$; $u(w_3, aq) = 0.0017$; $u(w_3, aq) = 0.30$; 0.27; $u(w_3, org) = 0.13$; $u(w_1, aq) = 1.1$; $u(w_2, aq) = 1.1$; $u(w_3, aq) = 0.000072$.

Table 3. Distribution coefficient of water (D_1) , distribution coefficient of ethanol (D_2) , and selectivity (S) from the experimental LLE data.^a The uncertainties inside the Table are standard deviations of the mean.

Method	Sample			
	Number	\mathbf{D}_1	D_2	S
Method 1	1	0.028 ± 0.002	0.352 ± 0.078	12.7 ± 3.3
	2	0.035 ± 0.009	0.170 ± 0.024	5.1 ± 1.6
	3	0.042 ± 0.010	0.214 ± 0.006	5.3 ± 1.4
	4	0.056 ± 0.010	0.229 ± 0.005	4.12 ± 0.77
	5	0.067 ± 0.002	0.238 ± 0.007	3.56 ± 0.19
	6	0.082 ± 0.01	0.267 ± 0.003	3.27 ± 0.49
	7	0.076 ± 0.060	0.278 ± 0.009	3.78 ± 0.95
	8	0.096 ± 0.008	0.291 ± 0.005	3.02 ± 0.27
	9	0.109 ± 0.006	0.279 ± 0.003	2.57 ± 0.15
	10	0.141 ± 0.016	0.324 ± 0.003	2.33 ± 0.28
Method 2	1	0.026 ± 0.005	0.60 ± 0.24	24 ± 14
	2	0.032 ± 0.005	0.173 ± 0.044	5.6 ± 2.5
	3	0.037 ± 0.005	0.182 ± 0.015	4.9 ± 1.1
	4	0.046 ± 0.006	0.233 ± 0.010	5.09 ± 0.63
	5	0.052 ± 0.006	0.259 ± 0.012	4.97 ± 0.42
	6	0.069 ± 0.009	0.255 ± 0.011	3.71 ± 0.51
	7	0.080 ± 0.015	0.259 ± 0.010	3.34 ± 0.76
	8	0.089 ± 0.011	0.259 ± 0.014	2.93 ± 0.37
	9	0.096 ± 0.010	0.261 ± 0.014	2.73 ± 0.31
	10	0.119 ± 0.010	0.278 ± 0.008	2.35 ± 0.24

^a The standard uncertainties are calculated by using the law of propagation of uncertainty. Standard uncertainties u are u(T) = 0.30 K; u(p) = 0.1 kPa; Method-1: $u(D_1) = 0.005$; $u(D_2) = 0.009$; u(S) = 0.51; Method-2: $u(D_1) = 0.005$; $u(D_2) = 0.026$; u(S) = 1.09.

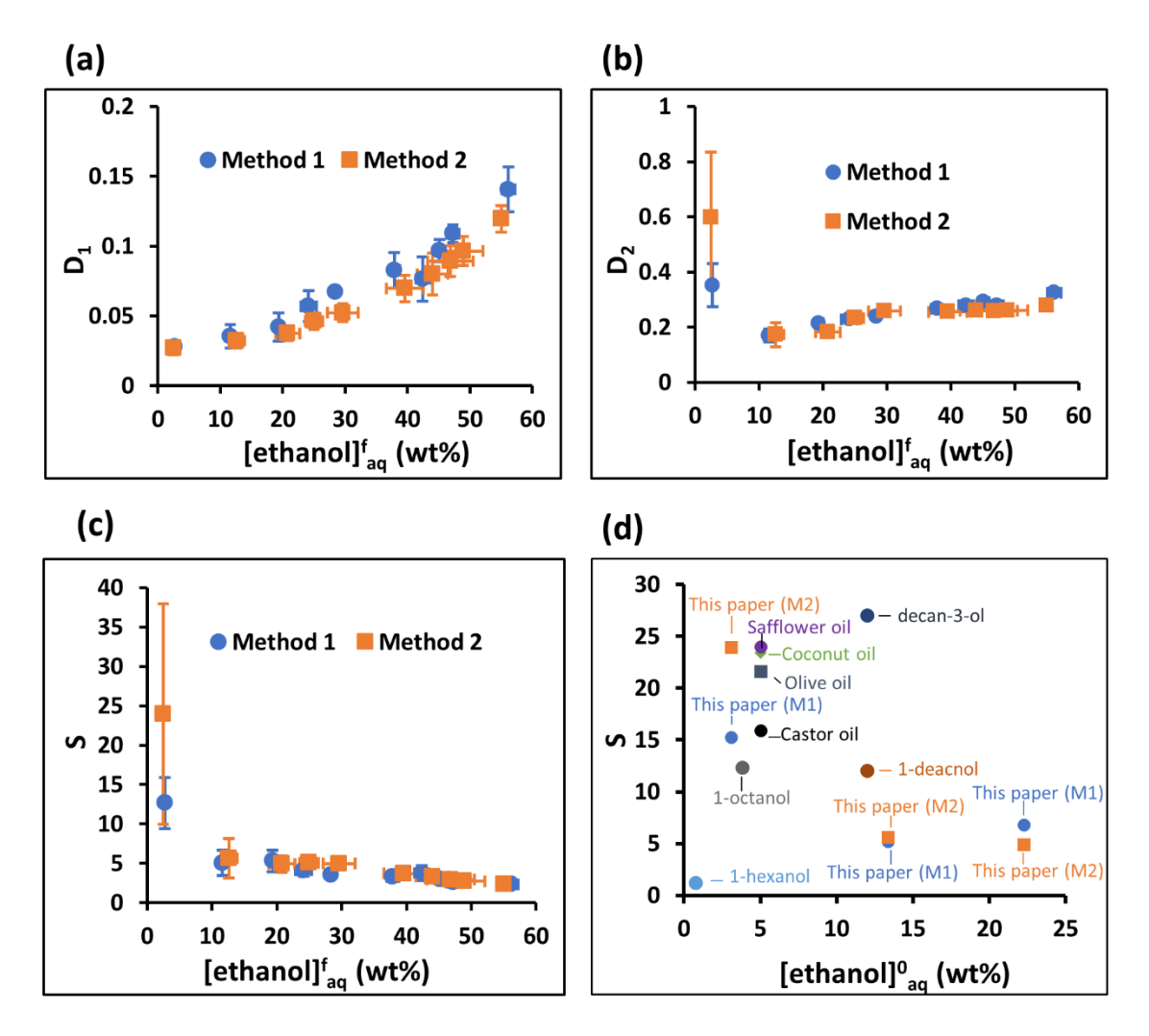


Figure 3. Graphs of (a) distribution coefficient of water, D_1 , (b) distribution coefficient of ethanol, D_2 , and (c) separation factor of ethanol, S, vs. final (equilibrium) aqueous phase ethanol concentration, [ethanol]^f_{aq}, using the experimental data obtained from HPLC Method 1 and Method 2. (d) Graphical comparison of the separation factors of ethanol obtained in this paper, with literature values, using castor oil [5], olive oil [5], coconut oil [5], safflower oil [5], 1-hexanol [6], 1-octanol [35], 1-deacnol [36], and decan-3-ol [36] at various initial aqueous ethanol concentration, [ethanol]⁰_{aq}.

Many researchers have reported separation factors for the extraction of ethanol using a variety of solvents [5,6,36]. Offeman et al. investigated a variety of vegetable oils such as castor oil, coconut oil, olive oil, and safflower oil to extract ethanol from an initial aqueous ethanol concentration, [ethanol]⁰_{aq}, of 5 wt% [5]. The separation factors of castor oil, coconut oil, olive oil, and safflower oil were found to be 15.9, 23.4, 21.6, and 24 respectively [5]. Keasler et al. tested a variety of C₁₀ alcohols as extractant solvents for recovering ethanol from an initial ethanol-water mixture of 12 wt% ethanol, and reported separation factors between 10 and 30 [36]. Munson et al. used a variety of C₆ to C₁₀ alcohols to extract ethanol from a 0.78 wt% bulk ethanol-water solution, and measured separation factors between 1.2 and 34 [6]. Offeman et al. measured the separation factor of ethanol at various concentrations (ranging from 0.73 to 15.4 wt%) in the aqueous phase using extractant solvents such as 1-nonanol, 1-decanol, 2-ethyl-1hexanol, 2-octanol and tributyl phosphate, and measured separation factors ranging from 10.5 to 19.7 [35]. Similarl, Pajak et al.

obtained ethanol separation factors of 7 and 8, at 5.02 and 7.08 wt%, respectively [37]. Note that the separation factor of ethanol at higher concentration (> 15.4 wt%) has rarely been studied. These high concentration values are needed to properly design multi-stage liquid-liquid extraction systems.

This work reports the separation factors of ethanol (S) at concentrations of 3 to 55 wt% in the aqueous phase, given in Table 3 and Figure 3, which were calculated from the distribution coefficients of water (D_1) and ethanol (D_2). Figure 3 shows D_1 increased with the equilibrium concentration of ethanol. While D_2 also increased with aqueous phase ethanol concentration at 11 wt% and higher, the opposite was observed when the concentration dropped to 3 wt%. The separation factor of ethanol (S), on the other hand, slightly decreased with increased ethanol concentration in the aqueous phase; it ranged from 12.67 to 2.41 and 22.18 to 2.33, for methods 1 and 2, respectively. The low concentration results are comparable to other published values with similar ethanol contents [5]. The experimentally measured high separation factors of ethanol at various ethanol concentrations in the aqueous phase suggest that castor oil is a good solvent to extract ethanol from water.

 Note that when ethanol was 2.5-2.7 wt % in the aqueous phase, the separation factor was highest for both methods, however the difference between the two methods was also very significant. Method 2 had an associated standard deviation of the mean of \pm 14 at 2.48 wt % ethanol, much higher than \pm 3.3 obtained for method 1 at a similar ethanol concentration of 2.73 wt %, mostly due to the reduced size of the castor oil peaks when they are separated in the HPLC column. However, in method 1 the oil components are combined into only 4 peaks giving rise to higher areas and are thus easier to detect. Therefore, HPLC method-1 provides more precise results. It is noted that Offeman et al. measured a separation factor of 15.9 at 5 wt% ethanol in the aqueous phase, which is in between our values at 3 wt%, and within the measured uncertainty[5].

3.3. Activity Coefficient Models

The UNIQUAC and NRTL models for liquid phase activity coefficients were fit to experimental liquidliquid equilibrium data sets to estimate the castor-oil pseudo-component in mixtures of ethanol, water and castor oil, using the natural-log form of the iso-activity equation:

336
$$\ln \gamma_{i,aq} + \ln x_{i,aq} = \ln \gamma_{i,org} + \ln x_{i,org}$$
 $i = 1 \dots C$ (4)

337 where $x_{i,p}$ is the mole fraction of species i in phase p and $\gamma_{i,p}$ is the activity coefficient of species i in phase p, as predicted by either the UNIQUAC or the NRTL model.

3.3.1. UNIQUAC Activity Coefficient Model

The UNIQUAC model for the activity coefficient of species i is:

$$342 \quad \ln \gamma_i = 1 - V_i + \ln V_i - \frac{z}{2} q_i \left(1 - \frac{V_i}{F_i} + \ln \left(\frac{V_i}{F_i} \right) \right) + q_i \left(1 - \ln \left(\frac{\sum_j q_j x_j \tau_{ji}}{\sum_j q_j x_j} \right) - \sum_j \frac{q_j x_j \tau_{ij}}{\sum_k q_k x_k \tau_{kj}} \right)$$
 (5)

$$V_i = \frac{r_i}{\sum_i r_i x_i} \tag{6}$$

$$344 F_i = \frac{q_i}{\sum_i q_i x_i} (7)$$

where q_i , V_i and F_i are the relative Van der Waals surface area, volume, volume fraction and surface fraction of species i, z is the coordination number, usually set to 10, and Δu_{ij} is the binary interaction parameter between species i and j.

The values of q_i , r_i , and Δu_{ij} for ethanol and water were obtained from the CHEMCAD database, while the remaining UNIQUAC parameters were fit to the experimental data sets obtained from each HPLC method. All predicted liquid-liquid equilibrium pairs passed the tangent plane stability test. The q_i and r_i parameters are given in Table 4 for water and ethanol, and in Table 5 for the fitted castor oil pseudocomponent. The Δu_{ij} binary interaction parameters are listed in Table 6.

Table 4. Van der Waals volume and surface area of water and ethanol from the CHEMCAD database.

Species	r_i	q_i
Water	0.92	1.3992
Ethanol	2.105	1.972

Table 5. Van der Waals fitted surface area and volume for the castor oil pseudo-component.

	Method 1	Method 2
R	29.7874	35.3277
Q	19.7272	20.4249

Table 6. UNIQUAC binary interaction parameters Δu_{ij} for {Water (1) + Ethanol (2) + Castor Oil (3)}.

Method 1						Method 2	
i∖j	Water	Ethanol	Castor Oil	i\j	Water	Ethanol	Castor Oil
Water	0	965.6218 a	1002.66	Water	0	965.6218 a	3659.53
Ethanol	212.6784a	0	-1389.55	Ethanol	212.6784 a	0	-1742.52
Castor Oil	195.04	3619.523	0	Castor Oil	-1466.48	4171.695	0

^a Parameter obtained from the CHEMCAD database.

3.3.2. NRTL Activity Coefficient Model

The NRTL model for the activity coefficient of species *i* is:

$$365 \qquad \ln \gamma_i = \frac{\sum_j \tau_{ji} G_{ji} x_j}{\sum_k G_{ki} x_k} + \sum_j \frac{G_{ij} x_j}{\sum_k G_{kj} x_k} \left[\tau_{ij} - \frac{\sum_k \tau_{kj} G_{kj} x_k}{\sum_k G_{kj} x_k} \right]$$

$$(9)$$

Here, $G_{ij} = \exp(-\alpha_{ij}\tau_{ij})$, where α_{ij} and τ_{ij} are experimentally fitted parameters. The values of α_{ij} and τ_{ij} at 295.15 K for ethanol and water were obtained from the CHEMCAD database, while all parameters involving the castor oil pseudo-component were fitted to the HPLC data. Tables 7 and 8 show the values for α_{ij} and τ_{ij} , respectively.

Table 7. NRTL parameter α_{ij} of binary pairs for {Water (1) + Ethanol (2) + Castor Oil (3)}.

	Method 1	Method 2
$\alpha_{1,2} = \alpha_{2,1}$	0.3031 a	0.3031 a
$\alpha_{1,3} = \alpha_{3,1}$	0.1275	0.1243
$\alpha_{2,3} = \alpha_{3,2}$	0.2698	0.2256

^a Parameter obtained from the CHEMCAD database.

Table 8. NRTL binary interaction parameters τ_{ij} for {Water (1) + Ethanol (2) + Castor Oil (3)}.

Method 1						Method 2	
i \ j	Water	Ethanol	Castor Oil	i∖j	Water	Ethanol	Castor Oil
Water	0	2.271349 a	43.4028	Water	0	2.271349 a	43.6208
Ethanol	-0.1869a	0	88.3423	Ethanol	-0.1869a	0	39.0507
Castor Oil	4.0821	1.6555	0	Castor Oil	3.3082	1.2839	0

^a Parameter obtained from the CHEMCAD database.

When the data from method 1 was fitted to the NRTL model, the solution converged to a metastable solution for two of the tie lines. Solving the iso-activity equations outside GAMS generated stable solutions to the liquid-liquid equilibrium problem. A better fit to this data could be achieved by adding a tangent plane stability cut to the least-squares fit optimization problem. Unfortunately, the GAMS license used for this work prevented solving the larger optimization problem.

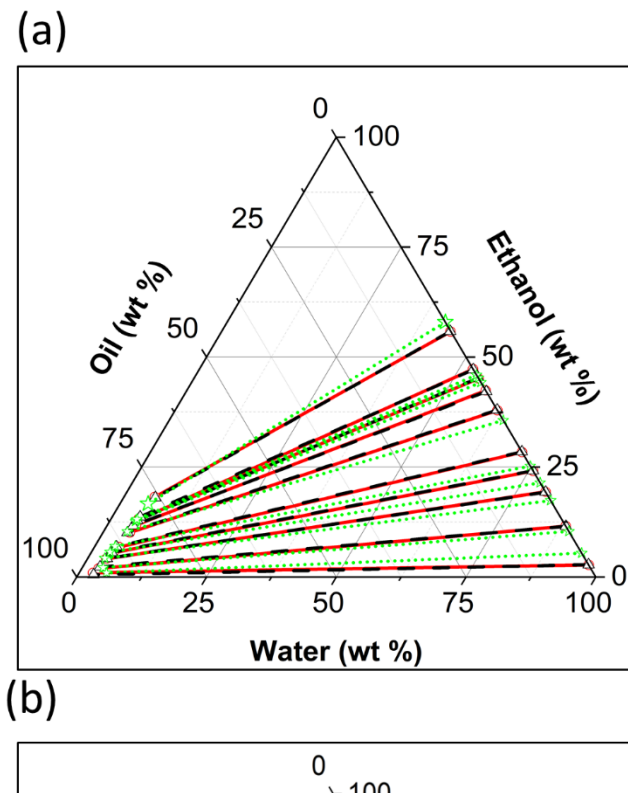
The ternary phase diagrams obtained from the experimental LLE data, the UNQUAC model (SM Table S4), and the NRTL model (SM Table S5) are represented in Figure 4. In addition, the UNIQUAC and NRTL results for both method-1 and method-2, were compared to the experimental data using the root mean square deviation (RMSD) [9]:

$$RMSD = \sqrt{\frac{\sum_{i=1}^{N} (w_i^{exp} - w_i^{model})^2}{N}}$$
Where, w_i^{exp} and w_i^{model} are the experimental and model weight percentage, i is any of the three

Where, w_i^{exp} and w_i^{model} are the experimental and model weight percentage, i is any of the three components such as water, ethanol, or castor oil, and N is the total number of data points which is 10 in all cases. As shown in Table 9, the RMSD of the UNIQUAC model ranged between 0.0199 to 0.612 wt% for method-1, and 0.0016 to 0.5098 wt% for method-2. The RMSD of the NRTL model ranged between 0.0196 to 2.104 wt% for method-1 and 0.001 to 1.9208 wt% for method-2. Overall, the average RMSD of the UNIQUAC model were found to be 0.245 wt% for method 1, and 0.332 wt% for method 2. These values were slightly smaller than those of the NRTL model, which were calculated to be 1.186 wt% and 0.6705 wt%, respectively. Thus, the results showed that the UNIQUAC model fitted the data better than the NRTL model for both methods 1 and 2. Note that the low RMSD values demonstrate that it is reasonable to treat castor oil as a pseudo-component in these models.

Table 9. RMSD values of UNIQUAC and NRTL model from experimental LLE data for {Water (1) + Ethanol (2) + Castor Oil (3)} at 295.15 K

Methods	Phase	Component	UNIQUAC (wt%)	NRTL (wt%)
Method 1	Aqueous phase	water	0.1114	2.1017
		ethanol	0.1079	2.1040
		castor oil	0.0199	0.0196
	Organic phase	water	0.6121	1.1260
		ethanol	0.258	0.5826
		castor oil	0.3590	1.1849
Method 2	Aqueous phase	Water	0.4743	1.9208
		ethanol	0.3964	1.8891
		castor oil	0.0016	0.0010
	Organic phase	water	0.1563	0.2536
		ethanol	0.4540	0.3580
		castor oil	0.5098	0.6006



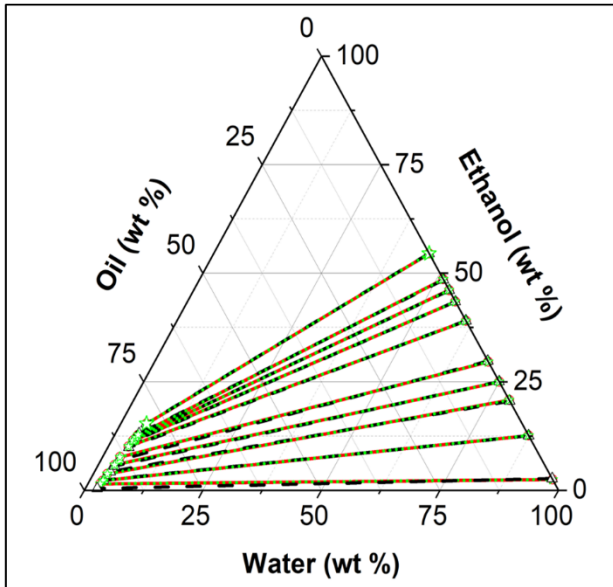


Figure 4. Ternary phase diagram of the ternary system {water + ethanol + castor oil} by using HPLC (a) Method 1; (b) Method 2 at T = 295.15 K and atmospheric pressure. Experimental data (red \circ , straight red tie lines), UNIQUAC data (black \triangle , dash tie lines), NRTL data (green \Rightarrow , dot tie lines)

3.4. Effect of CNC@Fe₃O₄ and lignin@Fe₃O₄ nanocomposites on LLE

The experimental LLE data of the ternary {water + ethanol + castor oil} system in the presence of CNC/Fe₃O₄ and lignin@Fe₃O₄ are listed in Tables 10 and 11, and shown in Figure 5. These were obtained using the HPLC method-1. The results showed that CNC@Fe₃O₄ has a very low (< 1%) or

negligible effect on the LLE data. Overall, CNC@Fe₃O₄ nanocomposites slightly increased the ethanol concentration in the organic phases, however, the differences of <1% were insignificant in practical terms. The average deviation of the newly developed LLE data in the presence of CNC@Fe₃O₄ compared to the data without nanoparticles ranged between 0.0045 to 0.7757 wt%. Similar results were seen for the measurements in the presence of lignin@Fe₃O₄. In this case, the ethanol concentration in the organic phase also increased by <1%, while the average deviation of the composition data ranged between 0.0018 to 0.7733 wt%. These results suggested that neither CNC@Fe₃O₄ nor lignin@Fe₃O₄ nanoparticles significantly adsorbed any of the three components, nor altered their chemical potentials. It is herein demonstrated for the first time that the NPs would not alter the thermodynamics of the liquid extraction process. As reported in previous publications [20,30], these NP have potential to stabilize Pickering emulsions for liquid extraction processes, while enabling magnetically controlled emulsion breakup and phase separation in the presence of an external magnetic field. Therefore, it is be proposed that the magnetic NPs can be used in three-component emulsion systems to stabilize dispersions formed during liquid extraction processes that accelerate mass transfer, but are usually problematic for macroscopic phase separation. However, these emulsions can be broken magnetically on demand to separate the aqueous and organic phases.

410

411

412 413

414

415

416

417 418

419

420 421

422

423

424 425

426

427

428 429

430

431

432

433

Table 10. Experimental LLE Mass (wt%) Obtained Using the HPLC for the Ternary System of {Water (1) + Ethanol (2) + Castor Oil (3)} at Temperature T = 295.15 K and at 101.2 kPa using the Method-1. CNC@Fe₃O₄ and lignin@Fe₃O₄ were utilized in the water/ethanol/castor oil ternary system to assist equilibrium. It is noted that w is mass percentage. The uncertainties inside the Table are standard deviations of the mean.

Nanoparticles	Organic phas	e		Aqueous phas	e	
	w_I	w_2	W3	w_I	w_2	W_3
CNC@Fe ₃ O ₄	2.79 ± 0.19	0.99 ± 0.11	96.22 ± 0.10	97.51 ± 0.19	2.49 ± 0.19	0.0016 ± 0.0002
	3.24 ± 0.15	2.05 ± 0.06	94.71 ± 0.09	88.79 ± 0.18	11.21 ± 0.18	0.0025 ± 0.0004
	3.77 ± 0.20	4.22 ± 0.03	92.01 ± 0.18	80.88 ± 0.20	19.12 ± 0.20	0.0029 ± 0.0004
	4.16 ± 0.16	5.75 ± 0.13	90.09 ± 0.14	76.1 ± 1.0	23.9 ± 1.0	0.0039 ± 0.0004
	4.79 ± 0.33	6.88 ± 0.15	88.33 ± 0.18	72.08 ± 0.53	27.91 ± 0.52	0.0049 ± 0.0005
	5.19 ± 0.31	10.27 ± 0.05	84.54 ± 0.32	62.44 ± 0.17	37.55 ± 0.17	0.0097 ± 0.0005
	5.65 ± 0.15	11.91 ± 0.04	82.44 ± 0.13	57.71 ± 0.21	42.29 ± 0.21	0.0020 ± 0.0002
	5.31 ± 0.25	13.28 ± 0.13	81.41 ± 0.12	55.24 ± 0.09	44.75 ± 0.09	0.0140 ± 0.0010
	4.92 ± 0.39	13.49 ± 0.34	81.59 ± 0.04	52.89 ± 0.26	47.09 ± 0.26	0.0190 ± 0.0017
	6.06 ± 0.36	18.37 ± 0.15	75.57 ± 0.23	45.39 ± 0.50	54.57 ± 0.49	0.0440 ± 0.0082
Lignin@Fe ₃ O ₄	2.92 ± 0.11	0.96 ± 0.02	96.12 ± 0.09	97.46 ± 0.08	2.54 ± 0.08	0.0015 ± 0.0005
	3.38 ± 0.14	2.01 ± 0.11	94.61 ± 0.06	88.34 ± 0.22	11.66 ± 0.22	0.0021 ± 0.0003
	3.66 ± 0.17	4.19 ± 0.10	92.15 ± 0.06	80.79 ± 0.19	19.21 ± 0.19	0.0026 ± 0.0002
	4.18 ± 0.20	5.71 ± 0.14	90.11 ± 0.11	75.97 ± 0.18	24.03 ± 0.18	0.0041 ± 0.0005
	4.91 ± 0.30	6.85 ± 0.11	88.24 ± 0.19	71.89 ± 0.30	28.11 ± 0.30	0.0051 ± 0.0006
	5.15 ± 0.28	10.19 ± 0.10	84.66 ± 0.19	62.32 ± 0.21	37.67 ± 0.21	0.0095 ± 0.0014
	5.66 ± 0.18	11.88 ± 0.12	82.46 ± 0.09	57.74 ± 0.21	42.25 ± 0.22	0.011 ± 0.011
	5.12 ± 0.21	13.33 ± 0.09	81.55 ± 0.13	55.11 ± 0.39	44.87 ± 0.39	0.0151 ± 0.0010
	5.02 ± 0.04	13.41 ± 0.10	81.57 ± 0.13	52.88 ± 0.09	47.10 ± 0.09	0.0232 ± 0.0020
	5.90 ± 0.35	18.43 ± 0.24	75.67 ± 0.11	45.40 ± 0.26	54.55 ± 0.25	0.0481 ± 0.0066

^a The standard uncertainties are calculated by using the law of propagation of uncertainty. Standard uncertainties u are u(T) = 0.30 K; u(p) = 0.1 kPa; $u(w_1, \text{ org}) = 0.33$; $u(w_2, \text{ org}) = 0.10$; $u(w_3, \text{ org}) = 0.31$; $u(w_1, \text{ aq}) = 0.48$, $u(w_2, \text{ aq}) = 0.48$; $u(w_3, \text{ aq}) = 0.0017$.

Nanoparticles	Sample	\mathbf{D}_1	D_2	S
	Number			
CNC@Fe ₃ O ₄	1	0.029 ± 0.002	0.398 ± 0.060	13.9 ± 3.2
	2	0.036 ± 0.002	0.183 ± 0.008	5.01 ± 0.48
	3	0.047 ± 0.003	0.221 ± 0.003	4.73 ± 0.33
	4	0.055 ± 0.003	0.240 ± 0.016	4.40 ± 0.48
	5	0.066 ± 0.005	0.246 ± 0.008	3.71 ± 0.37
	6	0.083 ± 0.005	0.273 ± 0.003	3.29 ± 0.21
	7	0.098 ± 0.003	0.282 ± 0.002	2.88 ± 0.11
	8	0.096 ± 0.005	0.297 ± 0.003	3.99 ± 0.19
	9	0.093 ± 0.008	0.286 ± 0.008	3.08 ± 0.33
	10	0.133 ± 0.009	0.337 ± 0.006	2.52 ± 0.23
Lignin@Fe ₃ O ₄	1	0.030 ± 0.001	0.378 ± 0.020	12.6 ± 1.1
	2	0.038 ± 0.002	0.17 ± 0.13	4.50 ± 0.53
	3	0.045 ± 0.002	0.218 ± 0.008	4.81 ± 0.41
	4	0.055 ± 0.003	0.238 ± 0.006	4.32 ± 0.33
	5	0.068 ± 0.004	0.244 ± 0.005	3.57 ± 0.29
	6	0.083 ± 0.005	0.270 ± 0.004	3.27 ± 0.23
	7	0.098 ± 0.003	0.281 ± 0.004	2.87 ± 0.14
	8	0.093 ± 0.004	0.297 ± 0.003	3.20 ± 0.17
	9	0.095 ± 0.001	0.285 ± 0.003	3.00 ± 0.01
	10	0.130 ± 0.008	0.338 ± 0.006	2.60 ± 0.22

^a The standard uncertainties are calculated by using the law of propagation of uncertainty. Standard uncertainties u are u(T) = 0.30 K; u(p) = 0.1 kPa; $u(D_1) = 0.005$; $u(D_2) = 0.009$; u(S) = 0.51.

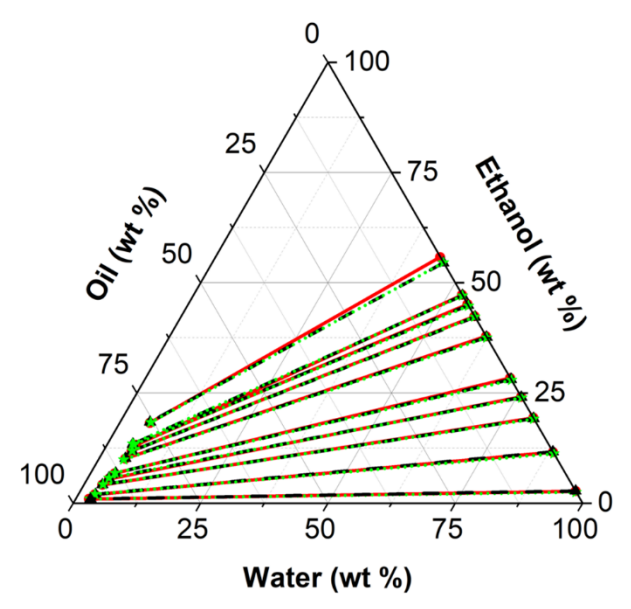


Figure 5. LLE ternary phase diagram of {water + ethanol + castor oil} at T = 295.15 K and atmospheric pressure in the presence of CNC@Fe₃O₄ and lignin@Fe₃O₄. No Nanoparticles (red \circ , straight red tie lines), CNC@Fe₃O₄ (black \triangle , black dash tie lines), lignin@Fe₃O₄ (green \rightleftharpoons , green dot tie lines)

4. Conclusion

The LLE of the ternary system {water + ethanol + castor oil} was measured using two HPLC methods at 295.15 K and at ambient pressure, to aid a future design of a liquid extraction system to purify dilute solutions of ethanol in water. For the purpose of liquid extraction, castor oil was proposed as an extractant solvent and was herein treated as a pseudo-component with a molecular weight approximately equal to the triglyceride of ricinoleic acid. Two HPLC methods were developed that only differed on the way the castor oil concentration was quantified. In method-1 most castor oil components were not separated and eluted together as 4 main peaks; while in method-2, several oil peaks were distinguished, but the 4 most prominent were used to quantify castor oil. Method-1 gave more precise results at low concentrations due to most castor oil components being overlapped into 4 major peaks.

Ternary diagrams were constructed by plotting the equilibrium compositions obtained with both analytical methods, and the data was fitted to the UNIQUAC and NRTL activity coefficient models. The results were used to obtain the van der Waals volume and surface area parameters of castor oil for the UNIQUAC model, in addition to the castor oil/water and castor oil/ethanol pair binary interaction parameters for both UNIQUAC and NRTL. Good agreements were obtained between fitted and experimental data with maximum root mean square deviations of 0.61% for UNIQUAC and 2.1% for NRTL. The separation factors and distribution coefficients of ethanol were calculated from the LLE data, resulting in high separation factors of 12.67 to 2.41, at aqueous phase ethanol concentrations ranging from 2.73 ± 0.35 to 55.82 ± 1.1 wt% according to method 1. These high values confirm that castor oil can be a suitable solvent to extract ethanol from water. Moreover, iron oxide-coated cellulose nanocrystals (CNC@Fe₃O₄) and Kraft lignin-coated iron oxide nanoparticles (lignin@Fe₃O₄) were introduced in the water/ethanol/castor oil mixtures to observe their impact on the LLE data. The results demonstrated that the nanoparticles had an insignificant effect (less than 1%) on the equilibrium. Therefore, CNC@Fe₃O₄ and lignin@Fe₃O₄ could be potentially used to control the formation of emulsions in liquid extraction systems without altering the thermodynamics of the purification process.

473

Funding

This work was funded in part by the National Science Foundation under Grants 1704897 and 1705331.

475

476

Notes

The authors declare no competing financial interest.

478

479

496

497

498

499

500

References

- 480 [1] S. Karimi, R.R. Karri, M. Tavakkoli Yaraki, J.R. Koduru, Processes and separation technologies for the production of fuel-grade bioethanol: a review, Environ Chem Lett. 19 (2021) 2873–2890. https://doi.org/10.1007/s10311-021-01208-9.
- 483 [2] B. Abdollahipoor, S.A. Shirazi, K.F. Reardon, B.C. Windom, Near-azeotropic volatility behavior of hydrous and anhydrous ethanol gasoline mixtures and impact on droplet evaporation dynamics, Fuel Processing Technology. 181 (2018) 166–174. https://doi.org/10.1016/j.fuproc.2018.09.019.
- 486 [3] Miranda Nahieh Toscano, Maciel Filho Rubens, Wolf Maciel Maria Regina, Comparison of Complete
 487 Extractive and Azeotropic Distillation Processes for Anhydrous Ethanol Production Using Aspen Plus
 488 Simulator, Chemical Engineering Transactions. 80 (2020) 43–48.
 489 https://doi.org/10.3303/CET2080008.
- 490 [4] A.J. Daugulis, D.B. Axford, P.J. McLellan, The economics of ethanol production by extractive fermentation, The Canadian Journal of Chemical Engineering. 69 (1991) 488–497. https://doi.org/10.1002/cjce.5450690213.
- 493 [5] R.D. Offeman, S.K. Stephenson, G.H. Robertson, W.J. Orts, Solvent extraction of ethanol from aqueous solutions using biobased oils, alcohols, and esters, J Amer Oil Chem Soc. 83 (2006) 153–157. https://doi.org/10.1007/s11746-006-1188-9.
 - [6] C.L. Munson, C.J. King, Factors influencing solvent selection for extraction of ethanol from aqueous solutions, Industrial & Engineering Chemistry Process Design and Development. 23 (1984) 109–115.
 - [7] G.D. Mehta, M.D. Fraser, A novel extraction process for separating ethanol and water, Industrial & Engineering Chemistry Process Design and Development. 24 (1985) 556–560. https://doi.org/10.1021/i200030a007.
- 501 [8] S. Ghosh, S.N. Mali, D.N. Bhowmick, A.P. Pratap, Neem oil as natural pesticide: Pseudo ternary diagram and computational study, Journal of the Indian Chemical Society. 98 (2021) 100088. https://doi.org/10.1016/j.jics.2021.100088.
- 504 [9] B.B. França, F.M. Pinto, F.L.P. Pessoa, A.M.C. Uller, Liquid-Liquid Equilibria for Castor Oil 505 Biodiesel + Glycerol + Alcohol, J. Chem. Eng. Data. 54 (2009) 2359–2364. 506 https://doi.org/10.1021/je800564d.
- 507 [10] H.M. Oliveira, L.R.S. Kanda, L.Z. Dante, M.L. Corazza, G.L. Sassaki, F.A.P. Voll, Liquid-liquid 508 equilibrium of systems containing acylglycerols from olive oil, glycerol and isopropanol, The Journal 509 of Chemical Thermodynamics. 165 (2022) 106666. https://doi.org/10.1016/j.jct.2021.106666.
- 510 [11] F.A.P. Voll, L.R.S. Kanda, L.C. Filho, M.L. Corazza, (Liquid+liquid) equilibrium for the system 511 (hydrolyzed palm oil+ethanol+water) for diacylglycerol enrichment, The Journal of Chemical 512 Thermodynamics. 58 (2013) 1–7. https://doi.org/10.1016/j.jct.2012.10.009.
- [12] V.R. Patel, G.G. Dumancas, L.C.K. Viswanath, R. Maples, B.J.J. Subong, Castor Oil: Properties,
 Uses, and Optimization of Processing Parameters in Commercial Production, Lipid Insights. 9 (2016)
 LPI.S40233. https://doi.org/10.4137/LPI.S40233.

- 516 [13] P.I. Nwabuokei, J.T. Nwabanne, The Effect of H2PO4 Catalyst on Biodiesel Production from Castor Seed Oil, International Journal of Progressive Sciences and Technologies. 22 (2020) 97–104. https://doi.org/10.52155/ijpsat.v22.1.1985.
- 519 [14] S. Thakur, N. Karak, Castor oil-based hyperbranched polyurethanes as advanced surface coating 520 materials, Progress in Organic Coatings. 76 (2013) 157–164. 521 https://doi.org/10.1016/j.porgcoat.2012.09.001.
- 522 [15] D.S. Ogunniyi, Castor oil: A vital industrial raw material, Bioresource Technology. 97 (2006) 1086– 523 1091. https://doi.org/10.1016/j.biortech.2005.03.028.
- 524 [16] M. Plante, C. Crafts, B. Bailey, I. Acworth, Characterization of castor oil by HPLC and charged aerosol detection, DIONEX. (2011) 1–5.
- [17] J.-T. Lin, J.M. Chen, L.P. Liao, T.A. McKeon, Molecular Species of Acylglycerols Incorporating
 Radiolabeled Fatty Acids from Castor (Ricinus communis L.) Microsomal Incubations, J. Agric. Food
 Chem. 50 (2002) 5077–5081. https://doi.org/10.1021/jf020454a.
- [18] S. Pradhan, C. Saha, M. Kumar, S.N. Naik, Transesterification and Reactive Extraction of Castor Oil for synthesis of Biodiesel/Biolubricant, IOP Conf. Ser.: Earth Environ. Sci. 785 (2021) 012005. https://doi.org/10.1088/1755-1315/785/1/012005.

534535

536

537 538

539 540

541

542 543

544

545

546

547 548

549

- [19] H. Mutlu, M.A.R. Meier, Castor oil as a renewable resource for the chemical industry, European Journal of Lipid Science and Technology. 112 (2010) 10–30. https://doi.org/10.1002/ejlt.200900138.
- [20] M.J. Hasan, F.A. Petrie, A.E. Johnson, J. Peltan, M. Gannon, R.T. Busch, S.O. Leontsev, E.S. Vasquez, E.E. Urena-Benavides, Magnetically induced demulsification of water and castor oil dispersions stabilized by Fe₃O₄-coated cellulose nanocrystals, Cellulose. 28 (2021) 4807–4823. https://doi.org/10.1007/s10570-021-03813-x.
- [21] F.A. Petrie, J.M. Gorham, R.T. Busch, S.O. Leontsev, E.E. Ureña-Benavides, E.S. Vasquez, Facile fabrication and characterization of kraft lignin@Fe3O4 nanocomposites using pH driven precipitation: Effects on increasing lignin content, International Journal of Biological Macromolecules. 181 (2021) 313–321. https://doi.org/10.1016/j.ijbiomac.2021.03.105.
- [22] L. Bai, S. Lv, W. Xiang, S. Huan, D.J. McClements, O.J. Rojas, Oil-in-water Pickering emulsions via microfluidization with cellulose nanocrystals: 1. Formation and stability, Food Hydrocolloids. 96 (2019) 699–708. https://doi.org/10.1016/j.foodhyd.2019.04.038.
- [23] L. Dai, Y. Li, F. Kong, K. Liu, C. Si, Y. Ni, Lignin-Based Nanoparticles Stabilized Pickering Emulsion for Stability Improvement and Thermal-Controlled Release of trans-Resveratrol, ACS Sustainable Chem. Eng. 7 (2019) 13497–13504. https://doi.org/10.1021/acssuschemeng.9b02966.
- [24] S. Parajuli, M.J. Hasan, E.E. Ureña-Benavides, Effect of the Interactions between Oppositely Charged Cellulose Nanocrystals (CNCs) and Chitin Nanocrystals (ChNCs) on the Enhanced Stability of Soybean Oil-in-Water Emulsions, Materials. 15 (2022) 6673. https://doi.org/10.3390/ma15196673.
- 551 [25] M.J. Hasan, this link will open in a new window Link to external site, Surface Modifications of 552 Cellulose Nanocrystals: Applications in Stabilization and Demulsification of Magnetically Controlled Castor Oil/Water/Ethanol Pickering Emulsions for Liquid-Liquid Extraction of Ethanol from Water, 553 554 Ph.D., The University of Texas San Antonio, https://www.proquest.com/docview/2702488214/90174A997A1B4D52PQ/1 (accessed August 23, 555 556 2022).
- [26] M.D. Wales, C. Huang, L.B. Joos, K.V. Probst, P.V. Vadlani, J.L. Anthony, M.E. Rezac, Liquid–Liquid Equilibria for Ternary Systems of Water + Methoxycyclopentane + Alcohol (Methanol, Ethanol, 1-Propanol, or 2-Propanol), J. Chem. Eng. Data. 61 (2016) 1479–1484. https://doi.org/10.1021/acs.jced.5b00803.
- [27] W.-L. Xue, C.-S. Zhang, Z.-X. Zeng, X.-H. Chen, Liquid–Liquid Equilibria for Systems of 1-Butanol
 + Water + 2,6-Diaminopyridine and 1-Butanol + Water + 2-Aminopyridine, J. Chem. Eng. Data. 54
 (2009) 1266–1270. https://doi.org/10.1021/je8007843.
- 564 [28] K. Wang, A.A.N.M. Al-Haimi, T. Zhang, J.A. Labarta, J. Gao, D. Xu, L. Zhang, Y. Wang, Explorations of Liquid–Liquid Phase Equilibrium for the Mixture (Isopropanol + Water) with

- Pyridinium-Based Ionic Liquids, J. Chem. Eng. Data. 66 (2021) 2192–2199. https://doi.org/10.1021/acs.jced.1c00066.
- 568 [29] M.J. Hasan, A.E. Johnson, E.E. Ureña-Benavides, "Greener" chemical modification of cellulose nanocrystals via oxa-Michael addition with N-Benzylmaleimide, Current Research in Green and Sustainable Chemistry. 4 (2021) 100081. https://doi.org/10.1016/j.crgsc.2021.100081.

573574

582 583

584

585

586

587 588

589

590 591

592

- [30] E.N. Westphal, Lignin-Magnetite Nanoparticles Aiding in Pickering Emulsions and Oil Manipulation and Their Rheological Properties, University of Dayton, 2021. https://etd.ohiolink.edu/apexprod/rws_olink/r/1501/10?clear=10&p10_accession_num=dayton1619 710097550949 (accessed July 31, 2022).
- [31] F. Dai, K. Xin, Y. Song, M. Shi, Y. Yu, Q. Li, Liquid-liquid equilibria for the ternary system 575 containing 1-Butanol + methoxy(methoxymethoxy)methane + water at temperatures of 303.15, 576 577 323.15 and 343.15 K, Fluid Phase Equilibria. 409 (2016)466-471. https://doi.org/10.1016/j.fluid.2015.11.009. 578
- 579 [32] H. Yan, Y. Han, S. Sun, M. Han, W. Fan, Q. Li, Liquid-liquid equilibrium for ternary systems of water + tetrahydrofurfuryl alcohol + isopentanol/1-hexanol at 303.2, 313.2, 323.2 K, The Journal of Chemical Thermodynamics. 166 (2022) 106688. https://doi.org/10.1016/j.jct.2021.106688.
 - [33] A. Yeboah, S. Ying, J. Lu, Y. Xie, H. Amoanimaa-Dede, K.G.A. Boateng, M. Chen, X. Yin, Castor oil (*Ricinus communis*): a review on the chemical composition and physicochemical properties, Food Sci. Technol. 41 (2020) 399–413. https://doi.org/10.1590/fst.19620.
 - [34] S.T. Keera, S.M. El Sabagh, A.R. Taman, Castor oil biodiesel production and optimization, Egypt J Pet. 27 (2018) 979–984. https://doi.org/10.1016/j.ejpe.2018.02.007.
 - [35] R.D. Offeman, S.K. Stephenson, G.H. Robertson, W.J. Orts, Solvent Extraction of Ethanol from Aqueous Solutions. I. Screening Methodology for Solvents, Industrial & Engineering Chemistry Research. 44 (2005) 6789–6796. https://doi.org/10.1021/ie0500319.
 - [36] S.J. Keasler, J.L. Lewin, J.I. Siepmann, N.M. Gryska, R.B. Ross, N.E. Schultz, M. Nakamura, Molecular insights for the optimization of solvent-based selective extraction of ethanol from fermentation broths, AIChE Journal. 59 (2013) 3065–3070. https://doi.org/10.1002/aic.14055.
- 593 [37] P. M, W. S, G. L, Liquid-liquid equilibrium in the system ethanol water tributyl phosphate toluene, 594 Inz. Chemiczna Proces. 18 (1997) 269–277.